

Anisotropies in thermal Casimir interactions: Ellipsoidal colloids trapped at a fluid interface

Ehsan Noruzifar and Martin Oettel

Institut für Physik, Johannes-Gutenberg-Universität Mainz, WA 331, 55099 Mainz, Germany

(Received 25 February 2009; published 8 May 2009)

We study the effective interaction between two ellipsoidal particles at the interface of two fluid phases which are mediated by thermal fluctuations of the interface. In this system the restriction of the long-ranged interface fluctuations by particles gives rise to fluctuation-induced forces which are equivalent to interactions of Casimir type and which are anisotropic in the interface plane. Since the position and the orientation of the colloids with respect to the interface normal may also fluctuate, this system is an example of the Casimir effect with fluctuating boundary conditions. In the approach taken here, the Casimir interaction is rewritten as the interaction between fluctuating multipole moments of an auxiliary charge-density-like field defined on the area enclosed by the contact lines. These fluctuations are coupled to fluctuations of multipole moments of the contact line position (due to the possible position and orientational fluctuations of the colloids). We obtain explicit expressions for the behavior of the Casimir interaction at large distances for arbitrary ellipsoid aspect ratios. If colloid fluctuations are suppressed, the Casimir interaction at large distances is isotropic, attractive, and long ranged (double logarithmic in the distance). If, however, colloid fluctuations are included, the Casimir interaction at large distances changes to a power law in the inverse distance and becomes anisotropic. The leading power is 4 if only vertical fluctuations of the colloid center are allowed, and it becomes 8 if also orientational fluctuations are included.

DOI: [10.1103/PhysRevE.79.051401](https://doi.org/10.1103/PhysRevE.79.051401)

PACS number(s): 82.70.Dd, 68.03.Kn

I. INTRODUCTION

When a fluctuating medium with long-ranged power-law correlations is confined between a set of boundaries, forces with likewise long-ranged character are induced between the boundaries. There are different possible sources of such fluctuations in a medium: in a quantum-mechanical system it is the zero-point energy of the vacuum (or ground state), and in a classical system it is the finite temperature which causes order-parameter fluctuations [1].

This kind of force was discovered theoretically by Casimir [2] in 1948 in the case of two parallel conductive and uncharged plates immersed in vacuum which he attributed to zero-point fluctuations of the electromagnetic field. For a review on recent progress and the status of experimental verification of this quantum-mechanical Casimir effect, see Ref. [3]. A classical equivalent of the Casimir force observable between objects immersed in a fluid in the vicinity of its critical point was predicted 30 years later [4]. The fluctuations of the order-parameter field near the critical point are long ranged, and thus they give rise to a Casimir-type fluctuation-induced force. This effect has recently been observed in an experiment probing the force on colloidal particles which have been immersed in a near-critical binary mixture in the vicinity of a wall [5]. Another classical variant of the Casimir interaction is found between particles (colloids) that are trapped at membranes [6,7] or at the interface of two fluid phases [1]. In this two-dimensional (2D) latter instance, thermally excited height fluctuations of the interface which have long-ranged nature are disturbed by the presence of colloids. The energy spectrum of the fluid interface on a coarse-grained level is very well described by an effective capillary-wave Hamiltonian which governs both the equilibrium interface configuration and the thermal fluctuations around this equilibrium. Since capillary waves are the

Goldstone modes of the broken translational symmetry pertaining to a free interface, their correlations decay logarithmically in the absence of gravity and the corresponding fluctuation-induced forces are a manifestation of the Casimir effect for a Gaussian theory in two dimensions. Compared to manifestations of the Casimir effect in a three-dimensional bulk medium, a new phenomenon arises here: the boundary of the fluctuating interface, which is represented by the contact line on the colloid surface, is itself mobile due to position fluctuations of the colloids and finite surface tensions of the colloid-liquid interfaces. Thus the Casimir force receives another contribution due to these fluctuating boundaries. This effect has been noticed first for colloidal rods trapped at membranes and films [7]. For a system composed of two spherical colloids trapped at a fluid interface, various realizations of these fluctuating boundary conditions are possible. It has been shown [8–10] that the fluctuation-induced force sensitively depends on the type of boundary conditions, with the asymptotics of the force ranging from $1/(d \ln d)$ to d^{-9} .

In recent work, the general form of the fluctuation-induced interactions between a finite number of compact objects of arbitrary shapes and separations has been calculated for a fluctuating medium of scalar Gaussian type [11] and an electromagnetic medium [12] with fixed boundary conditions on the surface of the objects. This has been achieved by viewing the Casimir interaction as resulting from fluctuations of source distributions (of the fluctuating field) on the surfaces of the objects which are decomposed in terms of multipoles. Then by a functional integral over the effective action of multipoles, the resulting interaction has been found. In such a way, the effect of anisotropic object shape on the Casimir force appears to be tractable. However, the objects' shape and the boundary conditions enter the effective action by its scattering matrix, which is a nontrivial object already for simple shapes [11]. Studies with explicit calculations for objects other than spheres, cylinders, and walls have partially

been focused on the effect of wall corrugations [13,14], but also sharp edges [15] and rectangular bodies [16] have been investigated. Also, in a recent work, the quantum Casimir interaction between two ellipsoidal particles as well as an ellipsoidal particle and a plane has been studied [17]. In the present work, we investigate the fluctuation-induced interactions between two ellipsoidal colloids that are trapped at the interface of two fluid phases with special emphasis on the effect of anisotropy. Ellipsoids (spheroids) of varying aspect ratios allow a smooth interpolation between spheres [8] and rods [7]. The ellipsoidal colloids are assumed to be of Janus type; therefore the interface contact line is always pinned to the colloids surface. Nevertheless the vertical position of colloids and their orientation may fluctuate, giving rise to the already mentioned feature of fluctuating boundaries. For the calculation of the Casimir force, we employ techniques which have been introduced in previous work [7–9] and which partially can also be interpreted in terms of the scattering matrix ansatz of Refs. [11,12] such that our results are a concrete example of the general theory for the effects of anisotropic object shape. As stressed before, however, at an interface we always have the influence of the fluctuating boundary conditions. In order to study the effect of the mobile boundaries in our work, we have divided our investigations into two main parts: an interface fluctuation part and a second part where the colloid fluctuations are included. In the interface fluctuation part, the positions of the colloids and thus the contact lines are fixed and therefore the problem reduces to the “usual” Casimir problem with Dirichlet boundary conditions. The Casimir interaction is determined by multipoles of an auxiliary field on the one-dimensional (1D) contact lines which is similar to the source field in the language of Ref. [11]. In the second part, we consider that the colloid position may fluctuate in all possible ways (height and tilts) which turns out to lead to Casimir interactions determined by multipoles of an auxiliary field defined on the 2D domain enclosed by the contact lines. The fluctuating boundaries result in certain restrictions on these multipoles. (Incidentally, we note that for small fluctuation amplitudes, an exact separation of interface and colloid fluctuation in the partition sum is possible [8,9]. This route, however, appears to be very difficult to follow for other than spherical colloids and is not taken here.)

The paper is structured as follows. In Sec. II, we introduce the effective Hamiltonian of the model system and the partition function which is defined by functional integrals over colloid and interface fluctuations. The implementation of the different boundary conditions is discussed. In Sec. III, we determine the fluctuation-induced force for the interface fluctuation part in the long- and short-distance regimes analytically and for intermediate distances numerically, respectively. In Sec. IV, we include the colloid fluctuations to the problem and discuss the modified long-distance asymptotics of the Casimir interaction. Section V contains a brief summary. Some technical details of the calculations have been relegated to Appendixes A and D.

II. MODEL

The investigated system consists of two nano- or microscopic uncharged spheroidal colloids with principal axes a

and a, b, b ($a > b$), which are trapped at the interface of two fluid phases I and II. The effective interaction between the colloids is mediated by thermal height fluctuations of the (sharp) interface. Without fluctuations, the equilibrium interface is flat and is set to be at $z=0$. The corresponding equilibrium position of the colloids is assumed to be symmetrical with respect to $z \rightarrow -z$, such that at the contact line the contact angle is $\pi/2$. The elliptic cross section of the ellipsoids with the equilibrium interface is denoted by $S_{i,\text{ref}}$ which is an ellipse with major and minor axes a and b , respectively. $S_{i,\text{ref}}$ may also be expressed in confocal elliptic coordinates by the elliptic radius ξ_0 ; see Appendix A for the coordinate definitions. The equilibrium interface at $z=0$ without the two elliptic holes $S_{i,\text{ref}}$ cut out by the colloids is termed the reference meniscus $S_{\text{men,ref}} = \mathbb{R}^2 \setminus \cup_i S_{i,\text{ref}}$. Deviations from this planar reference meniscus are considered to be small, without overhangs and bubbles. Therefore the Monge representation $(x, y, z = u(x, y)) = (\mathbf{x}, z = u(\mathbf{x}))$ is employed to describe the interface position. The colloids are of Janus type; thus the contact line is always pinned to their surface. The total Hamiltonian of the system which is used for calculating the free-energy costs of thermal fluctuations around the flat interface are determined by the change in interfacial energy of the interface I/II:

$$\begin{aligned} \mathcal{H}_{\text{tot}} &= \gamma \Delta A_{\text{men}} \\ &= \gamma \int_{S_{\text{men}}} d^2x \sqrt{1 + (\nabla u)^2} - \gamma \int_{S_{\text{men,ref}}} d^2x \\ &\approx \frac{\gamma}{2} \int_{S_{\text{men,ref}}} d^2x (\nabla u)^2 + \gamma \Delta A_{\text{proj}}, \end{aligned} \quad (1)$$

where $\gamma \Delta A_{\text{men}}$ expresses the energy needed for creating the additional meniscus area associated with the height fluctuations. In Eq. (1), S_{men} is the meniscus area projected onto the plane $z=0$ (where the reference interface is located) and $S_{\text{men,ref}}$ is the meniscus in the reference configuration mentioned above. The first equality in Eq. (1) constitutes the drumhead model which is well known in the renormalization-group analysis of interface problems, but is also used for the description of elastic surfaces (cf. Ref. [18]). In the second equality we have applied a small gradient expansion which is valid for slopes $|\nabla u| \ll 1$ and which provides the long-wavelength description of the interface fluctuations we are interested in. The small gradient expansion entails that

$$\Delta A_{\text{proj}} = \int_{S_{\text{men}} \setminus S_{\text{men,ref}}} d^2x \sqrt{1 + (\nabla u)^2} \approx \int_{S_{\text{men}} \setminus S_{\text{men,ref}}} d^2x \quad (2)$$

is the change in projected meniscus area with respect to the reference configuration. We rewrite this change in projected meniscus area in terms of the interface position $f_i = u(\partial S_{i,\text{ref}})$ at the reference contact line ellipses $\partial S_{i,\text{ref}}$. f_i corresponds (in second-order approximation) to the contact line of the colloid i with fluctuating center position h_i and fluctuating orientation. The contact line which is a function of the elliptic angle η only (see Appendix A for the definition of elliptic coordinates) is expanded as

$$f_i = u(\partial S_{i,\text{ref}}) = \sum_{m=0} [P_{im} \cos(m\eta_i) + Q_{im} \sin(m\eta_i)], \quad (3)$$

and we refer to the coefficients P_{im} and Q_{im} as boundary multipole moments below. The desired expression of ΔA_{proj} in terms of boundary multipole moments proceeds as discussed in Ref. [19] and allows us to identify it as a sum over boundary Hamiltonians $\mathcal{H}_{i,b}$ for each colloid i (see also Appendix B):

$$\gamma \Delta A_{\text{proj}} \equiv \sum_i \mathcal{H}_{b,i}[f_i] = \sum_i \frac{\pi\gamma}{2} (\tanh \xi_0 P_{i1}^2 + \coth \xi_0 Q_{i1}^2). \quad (4)$$

Putting Eqs. (1) and (4) together, the total change in interfacial energy is the sum

$$\mathcal{H}_{\text{tot}} = \mathcal{H}_{\text{cw}} + \mathcal{H}_{b,1} + \mathcal{H}_{b,2} = \frac{\gamma}{2} \int_{S_{\text{men,ref}}} d^2x (\nabla u)^2 + \mathcal{H}_{b,1} + \mathcal{H}_{b,2} \quad (5)$$

of the capillary-wave Hamiltonian \mathcal{H}_{cw} which describes the energy differences associated with the additional interfacial area over the reference configuration and the boundary Hamiltonians $\mathcal{H}_{b,i}$ which can be viewed as the energy cost due to fluctuations of the contact line (and which in turn are caused by colloid height and tilt fluctuations). As is well known, the Hamiltonian \mathcal{H}_{cw} is plagued with both a short-wavelength and a long-wavelength divergence which, however, can be treated by physical cutoffs. The natural short-wavelength cutoff is set by the molecular length scale σ of the fluid at which the capillary-wave model ceases to remain valid. The long-wavelength divergence is reminiscent of the fact that the capillary waves are Goldstone modes. Of course, in real systems the gravitational field provides a natural damping for capillary waves. Accounting also for the costs in gravitational energy associated with the interface height fluctuations, therefore, introduces a long-wavelength cutoff and leads to an additional term (“mass term”) in the capillary-wave Hamiltonian,

$$\mathcal{H}_{\text{cw}} = \frac{\gamma}{2} \int_{S_{\text{men,ref}}} d^2x \left[(\nabla u)^2 + \frac{u^2}{\lambda_c^2} \right]. \quad (6)$$

Here the capillary length is given by $\lambda_c = [\gamma / (|\rho_{\text{II}} - \rho_{\text{I}}|g)]^{1/2}$, where ρ_i is the mass density in phase i and g is the gravitational constant. Usually, in simple liquids, λ_c is in the range of millimeters and, therefore, is by far the longest length scale in the system. In fact, here it plays the role of a long-wavelength cutoff of the capillary-wave Hamiltonian \mathcal{H}_{cw} , and we will discuss our results in the limit $\lambda_c \gg R$ and $\lambda_c \gg d$. However, as we will see below, care is required when taking the limit $\lambda_c \rightarrow \infty$ (corresponding to $g \rightarrow 0$), since logarithmic divergences appear [20]. Another common way to introduce a long-wavelength cutoff is the finite size L of any real system. As discussed in Ref. [19], the precise way of incorporating the long-wavelength cutoff is unimportant for the effects on the colloidal length scale. As an example, in both approaches the width of the interface related to the capillary wave is logarithmically divergent, $\langle u(0)^2 \rangle$

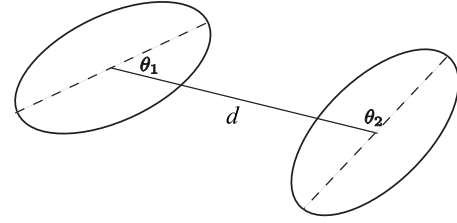


FIG. 1. Top view on the system.

$\sim \ln \lambda_c[L]/\sigma$. Via the integration domain of \mathcal{H}_{cw} , the total Hamiltonian of the system [Eq. (5)] implicitly depends on the geometric configuration. This leads to a free energy $\mathcal{F}(d, \theta_1, \theta_2)$ which depends on the distance d between the colloid centers and the orientation angles θ_1 and θ_2 of their major axes with respect to the distance vector joining the colloid centers (see Fig. 1). The free energy is related to the partition function $\mathcal{Z}(d, \theta_1, \theta_2)$ of the system by

$$\mathcal{F}(d, \theta_1, \theta_2) = -k_B T \ln \mathcal{Z}(d, \theta_1, \theta_2). \quad (7)$$

The partition function is obtained by a functional integral over all possible interface configurations u and boundary configurations f_i . The relation between interface and boundary configurations is included by δ -function constraints,

$$\mathcal{Z} = \mathcal{Z}_0^{-1} \int \mathcal{D}u \exp \left\{ -\frac{\mathcal{H}_{\text{cw}}[u]}{k_B T} \right\} \prod_{i=1}^2 \int \mathcal{D}f_i \prod_{\mathbf{x}_i \in \partial S_{i,\text{ref}}} \delta[u(\mathbf{x}_i) - f_i(\mathbf{x}_i)] \exp \left\{ -\frac{\mathcal{H}_{b,i}[f_i]}{k_B T} \right\}. \quad (8)$$

Here \mathcal{Z}_0 is a normalization factor such that $\mathcal{Z}(d \rightarrow \infty) = 1$ and ensures a proper regularization of the functional integral. Via the δ functions the interface field u is coupled to the contact line height f_i . Therefore, the boundary Hamiltonians $\mathcal{H}_{i,b}$ have a crucial influence on the resulting effective interaction between the colloids.

The kind of possible contact line fluctuations f_i is solely determined by the colloid fluctuations since the contact line is pinned. These fluctuations are vertical fluctuation of the colloids on the axis normal to the equilibrium interface (height) and orientational fluctuations around that axis (tilts) (Fig. 2). In order to incorporate various boundary conditions into the solutions, we categorize them into three cases:

(A) Colloids are fixed in the reference configuration; thus there are no integrations over the boundary terms.

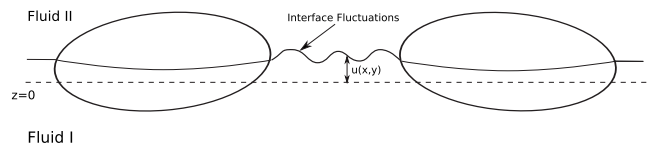


FIG. 2. Side view on the system.

(B) Colloid heights fluctuate freely without tilting; thus the boundary monopoles must be included in the integration measure so that $\mathcal{D}f_i = dP_{i0}$.

(C) There are unconstrained height and tilt fluctuations. Up to second order in the tilts this corresponds to the inclusion of boundary dipoles in the integration measure. Thus $\mathcal{D}f_i = dP_{i0}dP_{i1}dQ_{i1}$.

Case A corresponds to the “standard” Casimir effect in two dimensions with Dirichlet boundary conditions $f_i = u(\partial S_{i,\text{ref}}) = 0$. We call this the interface fluctuation part and it will be treated in Sec. III. Note that a short summary of this part was already given in Ref. [21]. The inclusion of the colloid height and tilt fluctuations in B and C is given in Sec. IV.

III. INTERFACE FLUCTUATION PART

The partition function \mathcal{Z}_{in} for fixed contact lines $f_i=0$ is given by

$$\mathcal{Z}_{\text{in}} = \mathcal{Z}_0^{-1} \int \mathcal{D}u \prod_{i=1}^2 \prod_{\mathbf{x}_i \in \partial S_{i,\text{ref}}} \delta(u(\mathbf{x}_i)) \exp \left\{ -\frac{\mathcal{H}_{\text{cw}}[u]}{k_B T} \right\}. \quad (9)$$

The disappearance of the interface fluctuations at the colloid boundaries is included by the Dirac delta function. In this section, analytical expressions for the fluctuation-induced force in the intermediate asymptotic regime $a \ll d \ll \lambda_c$ are calculated. We express the δ functions in Eq. (9) by their integral representation via auxiliary fields $\psi_i(\mathbf{x}_i)$ defined on the reference contact lines $\partial S_{i,\text{ref}}$. This enables us to integrate out the field u , leading to

$$\mathcal{Z}_{\text{in}} = \mathcal{Z}_0'^{-1} \int \prod_{i=1}^2 \mathcal{D}\psi_i \exp \left\{ -\frac{k_B T}{2\gamma} \sum_{i,j=1}^2 \int_{\partial S_{i,\text{ref}}} d\ell_i \int_{\partial S_{j,\text{ref}}} d\ell_j \psi_i(\mathbf{x}_i) G(|\mathbf{x}_i - \mathbf{x}_j|) \psi_j(\mathbf{x}_j) \right\}, \quad (10)$$

where $d\ell_i$ is the infinitesimal line segment on the circles $\partial S_{i,\text{ref}}$. After this integration, the normalization factor is changed, $\mathcal{Z}_0 \rightarrow \mathcal{Z}_0'$, such that still $\mathcal{Z}_{\text{in}}(d \rightarrow \infty) = 1$ holds. In Eq. (10) we introduced the Green’s function of the operator $(-\Delta + \lambda_c^{-2})$, which is given by $G(\mathbf{x}) = K_0(|\mathbf{x}|/\lambda_c)/2\pi$, where K_0 is the modified Bessel function of the second kind. In the range $d/\lambda_c \ll 1$ and $r_0/\lambda_c \ll 1$, we can use the asymptotic form of the K_0 for small arguments, such that $2\pi G(|\mathbf{x}|) \approx -\ln(\gamma_e |\mathbf{x}|/2\lambda_c)$. Here, $\gamma_e \approx 1.781\,972$ is the Euler-Mascheroni constant exponentiated. We introduce auxiliary multipole moments as the Fourier transforms of the auxiliary fields ψ_i on the reference contact line $\partial S_{i,\text{ref}}$,

$$\begin{aligned} \hat{\psi}_{im}^c &= \int_0^{2\pi} d\eta_i h(\eta_i) \cos(m\eta_i) \psi_i(\mathbf{x}_i(\eta_i)), \\ \hat{\psi}_{im}^s &= \int_0^{2\pi} d\eta_i h(\eta_i) \sin(m\eta_i) \psi_i(\mathbf{x}_i(\eta_i)), \end{aligned} \quad (11)$$

where η_i is the elliptic angle pertaining to a coordinate system centered around each colloid i , respectively, such that

the x axis in this colloid-specific coordinate system joins the two foci of $S_{i,\text{ref}}$. Furthermore, $h(\eta_i)$ is the scale factor in elliptic coordinates (see Appendix A). The lengthy calculation leading to the multipole (Fourier) decomposition for the Green’s function $G(|\mathbf{x}_i - \mathbf{x}_j|)$ (for general orientations θ_1 and θ_2 of the ellipsoids) is given in Appendix C. The final results are collected in Eqs. (C1) and (C15)–(C17). Using this, the double integral in the exponent of Eq. (10) can be written as a double sum over the auxiliary multipole moments (Fourier components), consisting of a self-energy part G_{self} when x_i and x_j reside on one ellipse and G_{int} when the points x_i and x_j reside on different ellipses. The functional integral over the auxiliary fields becomes a product of integrals over their multipole moments, $\mathcal{D}\psi_i = d\hat{\psi}_{i0} \prod_{j=1}^{\infty} d\hat{\psi}_{ij}^c d\hat{\psi}_{ij}^s$, and the resulting partition function then reads

$$\mathcal{Z}_{\text{in}} = \mathcal{Z}_0'^{-1} \int \prod_{i=1}^2 \mathcal{D}\hat{\Psi}_i \exp \left\{ -\frac{k_B T}{2\gamma} \begin{pmatrix} \hat{\Psi}_1 \\ \hat{\Psi}_2 \end{pmatrix}^T \begin{pmatrix} \hat{\mathbf{G}}_{\text{self}} & \hat{\mathbf{G}}_{\text{int}} \\ \hat{\mathbf{G}}_{\text{int}} & \hat{\mathbf{G}}_{\text{self}} \end{pmatrix} \begin{pmatrix} \hat{\Psi}_1 \\ \hat{\Psi}_2 \end{pmatrix} \right\}, \quad (12)$$

where the vectors $\hat{\Psi}_i = (\hat{\Psi}_i^c, \hat{\Psi}_i^s)$, with $\hat{\Psi}_i^c = (\hat{\psi}_{i0}^c, \hat{\psi}_{i1}^c, \dots)$ and $\hat{\Psi}_i^s = (\hat{\psi}_{i1}^s, \hat{\psi}_{i2}^s, \dots)$, contain the auxiliary multipole moments of colloid i . The coupling matrix $\hat{\mathbf{G}}$ which contains the Fourier modes of the Green’s function $G(\mathbf{x}_i - \mathbf{x}_j)$ has a block structure. The self-energy submatrix $\hat{\mathbf{G}}_{\text{self}}$ which describes the coupling between auxiliary moments of the same colloid are diagonal, and its form can be determined from definition (11) and Eq. (C1),

$$\begin{aligned} 2\pi (\hat{\Psi}_i^T \hat{\mathbf{G}}_{\text{self}} \hat{\Psi}_i) &= -\ln \frac{\gamma_e a' e^{\xi_0}}{8\lambda_c} (\hat{\psi}_{i0}^c)^2 + 2 \sum_{n=1}^{\infty} \frac{e^{-n\xi_0}}{n} \\ &\quad \times [\cosh(n\xi_0) (\hat{\psi}_{in}^c)^2 + \sinh(n\xi_0) (\hat{\psi}_{in}^s)^2], \end{aligned} \quad (13)$$

where $a'^2 = a^2 - b^2$. The off-diagonal blocks $\hat{\mathbf{G}}_{\text{int}}$ characterize the interaction between the multipole moments residing on different colloids. It is convenient to split the matrix into a block structure describing the interaction of cosine and sine multipoles:

$$2\pi (\hat{\Psi}_1^T \hat{\mathbf{G}}_{\text{int}} \hat{\Psi}_2) = \begin{pmatrix} \hat{\Psi}_1^c \\ \hat{\Psi}_1^s \end{pmatrix}^T \begin{pmatrix} \hat{\mathbf{G}}_{\text{int}}^{cc} & \hat{\mathbf{G}}_{\text{int}}^{sc} \\ \hat{\mathbf{G}}_{\text{int}}^{sc} & \hat{\mathbf{G}}_{\text{int}}^{ss} \end{pmatrix} \begin{pmatrix} \hat{\Psi}_2^c \\ \hat{\Psi}_2^s \end{pmatrix}. \quad (14)$$

The matrix elements of such defined submatrices follow from Eqs. (C15)–(C17), and are explicitly given by

$$(\hat{\mathbf{G}}_{\text{int}}^{cc})_{00} = -\ln \left(\frac{\gamma_e d}{2\lambda_c} \right), \quad (15)$$

$$(\hat{\mathbf{G}}_{\text{int}}^{cc})_{mn} = \sum_{l=0}^{\infty} \left(\frac{a'}{4d} \right)^{m+n+2l} A_{mnl}^c(\theta_1, \theta_2) \cosh(m\xi_0) \cosh(n\xi_0), \quad (16)$$

$$(\hat{\mathbf{G}}_{\text{int}}^{ss})_{mn} = - \sum_{l=0} \left(\frac{a'}{4d} \right)^{m+n+2l} A_{mnl}^c(\theta_1, \theta_2) \sinh(m\xi_0) \sinh(n\xi_0), \quad (17)$$

$$(\hat{\mathbf{G}}_{\text{int}}^{sc})_{mn} = \sum_{l=0} \left(\frac{a'}{4d} \right)^{m+n+2l} A_{mnl}^s(\theta_1, \theta_2) \sinh(m\xi_0) \cosh(n\xi_0). \quad (18)$$

From Eq. (12) we find that the fluctuation part of the free energy reads

$$\mathcal{F}_{\text{in}} = -k_B T \ln \mathcal{Z}_{\text{in}} = -\frac{k_B T}{2} \ln(\det \hat{\mathbf{G}}) + \text{const}, \quad (19)$$

where $\text{const} = -k_B T \ln \mathcal{Z}'_0$. The factors $A_{mnl}^{[s]}(\theta_1, \theta_2)$, given in Eqs. (C16) and (C17), contain the dependence on the orientation angles θ_1 and θ_2 of the ellipsoids (see Fig. 1). As can be seen from above, the interaction coefficients $(\hat{\mathbf{G}}_{\text{int}}^{[s][s]})_{mn}$ between multipoles of orders m and n take the form of a series in $1/d$, starting at $1/d^{m+n}$. (For spherical colloids, this multipole interaction coefficient only contains the order $1/d^{m+n}$ [9].) In principle, the matrix $\hat{\mathbf{G}}$ is infinite dimensional and $\det(\hat{\mathbf{G}})$ is divergent and its regularization is provided by the normalization factor \mathcal{Z}'_0 . The explicit series for the elements of $\hat{\mathbf{G}}_{\text{int}}$ allows for a systematic expansion of the logarithm in Eq. (19) in powers of $1/d$,

$$\mathcal{F}_{\text{in}}(d) = k_B T \sum_n f_{2n}^{\text{in}} \left(\frac{1}{d} \right)^{2n}, \quad (20)$$

where the coefficients f_{2n}^{in} depend on the logarithms $-\ln(\gamma_c d / 2\lambda_c)$ and $-\ln(\gamma_c a' e^{\xi_0} / 8\lambda_c)$, as well as the angles θ_1 and θ_2 . The number of auxiliary multipoles included in the calculation of the asymptotic form of $\mathcal{F}_{\text{fluc}}$ in Eq. (20) is determined by the desired order in $1/d$. Inclusion of multipoles up to order n leads to asymptotics correct up to $1/d^{2n}$. In the limit $\lambda_c/d \rightarrow \infty$ the free-energy expansion coefficients in Eq. (20) up to fourth order are¹

$$f_0^{\text{in}} = \frac{1}{2} \ln \left(\frac{4d}{a+b} \right) + \text{const},$$

$$f_2^{\text{in}} = - \frac{1}{2 \ln \left(\frac{4d}{a+b} \right)} \times \left[\frac{(a+b)^2}{16} + \frac{3}{32} (a^2 - b^2) [\cos(2\theta_1) + \cos(2\theta_2)] \right],$$

¹Note that a factor of $1/\{2 \ln[2d/(a+b)]\}$ is missing in the expression for f_2^{in} in Eq. (29) of Ref. [21].

$$f_4^{\text{in}} = - \frac{1}{2^{11}} \left\{ \frac{1}{\ln \left(\frac{4d}{a+b} \right)} \{ 16(a-b)(a+b)^3 [\cos(2\theta_1) + \cos(2\theta_2)] + 11(a^2 - b^2)^2 [\cos(4\theta_1) + \cos(4\theta_2)] + 44(a^2 - b^2)^2 \cos(2\theta_1 + 2\theta_2) + 6(a+b)^4 \} + [8(a^2 - b^2)^2 \cos(2\theta_1 + 2\theta_2) + 8(a+b)^4] \right\} - \frac{1}{2} (f_2^{\text{in}})^2 \quad (21)$$

The double-logarithmic divergence in d in the leading coefficient f_0^{in} is a reflection of the fact that the interface itself becomes ill defined for $\lambda_c \rightarrow \infty$ due to the capillary waves. For the Casimir force itself, however, we find a finite value for all d in the limit $\lambda_c \rightarrow \infty$. Anisotropies in the Casimir interaction appear here first in the subleading term f_2^{in} . Their angular dependence stems from the monopole-dipole interaction of the auxiliary field, and the attraction is maximal if both ellipses are aligned tip to tip.

In the opposite limit of small surface-to-surface distance $h = d - d_{cl} \ll d_{cl}$ (where d_{cl} is the distance of the closest approach between ellipses), the fluctuation force can be calculated by using the Derjaguin (or proximity) approximation [22]. It consists of replacing the local force density on the contact lines by the result for the fluctuation force per length $f_{2d}(\tilde{h})$ between two parallel lines with a separation distance \tilde{h} and integrating over the two opposite contact lines to obtain the total effective force between the colloids. The Casimir force density between two parallel surfaces was calculated in Ref. [23] in a general approach for arbitrary dimensions. Applied to two dimensions we obtain the force line density $f_{2d}(\tilde{h}) = -k_B T \pi / 24 \tilde{h}^2$. Integrating this density over the opposing contact lines yields [21]

$$F_{\text{in}} \approx - \frac{\pi k_B T}{24} \int_{-\infty}^{+\infty} dy \frac{1}{\left[h + \frac{y^2}{2} \left(\frac{1}{R_1} + \frac{1}{R_2} \right) \right]^2} = -k_B T \frac{\pi^2}{48 h^{3/2}} \sqrt{\frac{2}{\frac{1}{R_1} + \frac{1}{R_2}}} + \mathcal{O}(h^{-1/2}). \quad (22)$$

Here, R_1 and R_2 are the curvature radii of the two ellipses at the end points of the distance vector of the closest approach. It is seen that the fluctuation force diverges as $h^{-3/2}$ upon contact of the ellipsoids ($h \rightarrow 0$).

Intermediate distances: Numerical calculation

For intermediate distances $d - d_{cl} \approx a$, the fluctuation-induced force has to be calculated numerically. This can be done in principle by including a number of multipoles in the numeric evaluation of the determinant in Eq. (19); see Ref. [11]. In order to avoid the algebraic evaluation of the multipole coefficients of $\hat{\mathbf{G}}$, it is possible to apply a method which was introduced in Ref. [13]. The starting point is Eq. (10) for

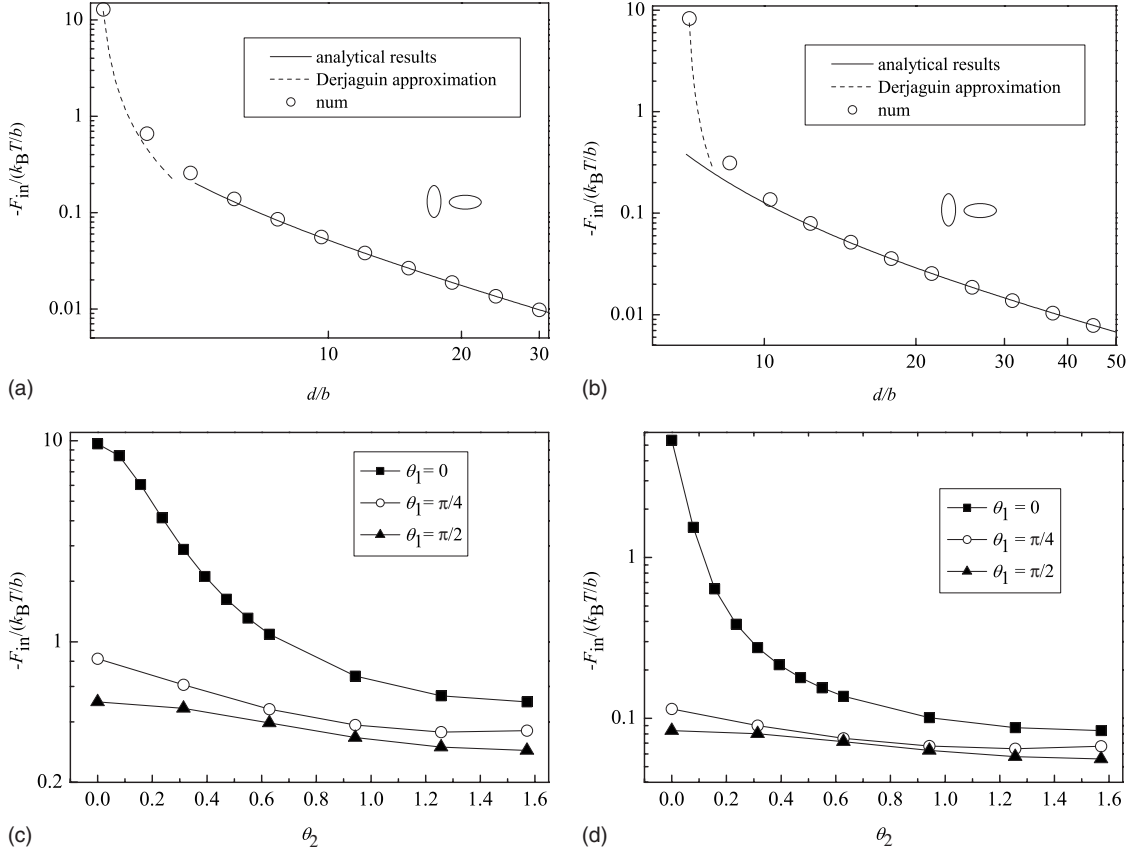


FIG. 3. [(a) and (b)] Comparison of the numerical results for the interface fluctuation Casimir force (symbols) with the analytical expressions in the asymptotic ranges of large colloid separations $d \gg a, b$ (full line) and small surface-to-surface distance $h = d - d_{cl} \ll b$ (dashed line). [(c) and (d)] Numerical Casimir interaction between two fixed ellipsoids trapped at the interface as a function of their orientation, for $d = 4.1$ and $d = 12.1$, respectively.

the partition function Z_{in} . Introducing a mesh with N points η_{ij} , with $j = 1, \dots, N$, on the reference contact line $\partial S_{i,\text{ref}}$ converts the double integral in the exponent to a double sum. Thus the functional integrals over the auxiliary fields $\psi_i(\eta_i)$ are replaced by ordinary Gaussian integrals over the $\psi_i(\mathbf{x}_i(\eta_{ij}))$, $\mathcal{D}\psi_i \equiv \prod_{j=0}^N d\psi_i(\mathbf{x}_i(\eta_{ij}))$. In the exponent, the $\psi_i(\mathbf{x}_i(\varphi_{ij}))$ are coupled by a matrix \mathbf{G} with elements $G_{ii'}^{jj'} = G(|\mathbf{x}_i(\eta_{ij}) - \mathbf{x}_{i'}(\eta_{i'j'})|)$. Performing the Gaussian integrals and disregarding divergent and d -independent terms immediately leads to $\mathcal{F}_{\text{in}} = (k_B T/2) \ln \det[\mathbf{G}_{\infty}^{-1} \mathbf{G}(d)]$ for the fluctuation free energy. Here, $\mathbf{G}_{\infty} \equiv \lim_{d \rightarrow \infty} \mathbf{G}(d)$. It contains the self-energy contributions and is needed for the regularization of the free energy. Deriving with respect to d , the Casimir force can be written as

$$F_{\text{in}}(d) = -\frac{k_B T}{2} \text{tr}[\mathbf{G}(d)^{-1} \partial_d \mathbf{G}(d)]. \quad (23)$$

The advantage of the direct calculation of the force is that Eq. (23) does not contain any divergent parts which would require regularization, thus easing the numerical treatment considerably. The determinant is computed by using a standard factorization into lower and upper triangular matrices for inversion [24]. We find good convergence of the numerical routine. The convergence can be sped up by distributing

more points in the regions where the ellipses face each other. We note that computing the force by the multipole series seems to be more efficient [11]. This can partially be compensated for by the point distribution on the ellipses. In Fig. 3(a) (ellipse aspect ratio: 2) and Fig. 3(b) (aspect ratio: 6), we compare the analytical results of Eq. (20) and the Derjaguin approximation [Eq. (22)] with the numerical results. As shown the analytical expressions show very good agreement with the numerical data points for both long- and short-range behaviors and almost cover the whole distance regime. At large distances d , the leading term of the free-energy expansion in Eq. (20) mainly determines the behavior of the Casimir interaction because of its long-ranged nature. Hence the orientation dependence of the subleading terms can be neglected. In order to demonstrate the anisotropy of the Casimir interaction, we show results for a fixed intermediate distance d between ellipsoid centers and varying orientation θ_2 of the second ellipsoid; see Fig. 3(c) (aspect ratio: 2; $d/b = 4.1$) and Fig. 3(d) (aspect ratio: 6; $d/b = 12.1$). The orientation of the first ellipse was fixed to three values, $\theta_1 = 0$, $\theta_1 = \pi/4$, and $\theta_1 = \pi/2$. As can be seen, the fluctuation-induced interaction is maximally attractive for $\theta_1 = \theta_2 = 0$ (tip-to-tip configuration). When θ_2 deviates from zero then the resulting force reduces. This behavior holds for both aspect ratios of 2 and 6.

IV. INCLUSION OF COLLOID FLUCTUATIONS

In general, the inclusion of colloid height and tilt fluctuations into the partition function [Eq. (8)] can be realized by an approach used in Refs. [8,9]. In this approach, the partition function is split into a product of a colloid fluctuation part and the interface fluctuation part. The latter contains only the contribution of the fluctuating interface, with Dirichlet boundary conditions on the colloid surface (see Sec. III). In the colloid fluctuation part, the fluctuations of colloid heights and tilts are weighted by a Boltzmann factor which contains the energy of the mean-field solution (Euler-Lagrange equation) to the capillary problem with the boundary conditions set by the fluctuating contact line. This decomposition is possible due to the fact that capillary-wave Hamiltonian is Gaussian in the field u . In principle, it is possible to use this method also for the special case of ellipsoidal colloids considered here. However, finding the mean-field solution in such a geometry for arbitrary contact lines is rather cumbersome. To bypass this difficulty, we employed a trick adapted from Ref. [7] in which effective forces between rods on fluctuating membranes and films have been investigated. We extend the fluctuating interface height field $u(x, y)$ which enters the functional integral for \mathcal{Z} to the interior of the ellipses $S_{i,\text{ref}}$. Thus the measure of the functional integral for \mathcal{Z} is extended by $Du(\mathbf{x})|_{\mathbf{x} \in S_{i,\text{ref}}}$ and the integration domain in the capillary-wave Hamiltonian is enlarged to encompass the whole \mathbb{R}^2 . On the colloid surfaces, the interface height field is given by the three-phase contact line, $u(\partial S_{i,\text{ref}}) \equiv f_i$. We extend u continuously to the interior of the circles $S_{i,\text{ref}}$. Such a continuation is not unique. However, the partition function remains unchanged (up to a constant factor), if the energy cost of such a continuation is zero (as physically required since the interface is pinned to the ellipsoid surface). This has to be ensured by appropriate counterterms [8,9]. We choose the continuation

$$\begin{aligned} u(S_{i,\text{ref}}) &\equiv f_{i,\text{ext}}(\xi_i, \eta_i) \\ &= \sum_m \left(P_{im} \frac{\cos(hm\xi_i)}{\cosh(m\xi_0)} \cos(m\eta_i) \right. \\ &\quad \left. + Q_{im} \frac{\sinh(m\xi_i)}{\sinh(m\xi_0)} \sin(m\eta_i) \right), \end{aligned} \quad (24)$$

where ξ_i and η_i are the elliptic coordinates with respect to ellipse $S_{i,\text{ref}}$. The specific choice above is convenient for the further calculations since $\nabla^2 f_{i,\text{ext}} = 0$ in $S_{i,\text{ref}} \setminus \partial S_{i,\text{ref}}$. Extending the integration domain of the capillary-wave Hamiltonian in Eq. (5), $\Omega = \mathbb{R}^2 \setminus \cup_i S_{i,\text{ref}} \rightarrow \mathbb{R}^2$ generates an additional energy contribution $-\mathcal{H}_{i,\text{corr}}$ which has to be subtracted from the extended capillary-wave Hamiltonian $\mathcal{H}_{\text{cw}}[\Omega \equiv \mathbb{R}^2]$. Therefore, the total Hamiltonian reads

$$\mathcal{H}_{\text{tot}} = \mathcal{H}_{\text{cw}} + \sum_{i=1}^2 [\mathcal{H}_{i,\text{b}} + \mathcal{H}_{i,\text{corr}}]. \quad (25)$$

The correction Hamiltonian is calculated in Appendix B, and we recall the boundary Hamiltonians

$$\begin{aligned} -\mathcal{H}_{i,\text{corr}} &= \frac{\gamma\pi}{2} \sum_m m [P_{im}^2 \tanh(m\xi_0) + Q_{im}^2 \coth(m\xi_0)], \\ \mathcal{H}_{i,\text{b}} &= \frac{\gamma\pi}{2} [P_{i1}^2 \tanh(\xi_0) + Q_{i1}^2 \coth(\xi_0)]. \end{aligned} \quad (26)$$

In Eq. (26) we have already omitted the contributions from the gravitational term in \mathcal{H}_{cw} which are of order $(a/\lambda)^2 \ll 1$.

As in Sec. III the partition function is written as a functional integral over all possible configurations of the interface position u and the boundary lines, expressed by f_i ,

$$\begin{aligned} \mathcal{Z} &= \mathcal{Z}_0^{-1} \int Du \prod_{i=1}^2 \int \mathcal{D}f_i \prod_{\mathbf{x}_i \in S_{i,\text{ref}}} \delta[u(\mathbf{x}_i) - f_{i,\text{ext}}(\mathbf{x}_i)] \\ &\quad \times \exp \left\{ -\frac{\mathcal{H}_{\text{tot}}[f_i, u]}{k_B T} \right\}, \end{aligned} \quad (27)$$

where the product over the δ functions enforces the pinning of the interface at the positions of the colloids. In contrast to Eq. (8), this product extends over all $\mathbf{x} \in S_{i,\text{ref}}$ instead of $\partial S_{i,\text{ref}}$ only. The δ functions can again be expressed by auxiliary fields ψ_i , now defined on the *two-dimensional* elliptical domains $S_{i,\text{ref}}$ as opposed to the auxiliary fields of Sec. III, which are defined on the *one-dimensional* ellipses $\partial S_{i,\text{ref}}$:

$$\begin{aligned} \mathcal{Z} &= \int Du \int \prod_{i=1}^2 \mathcal{D}\psi_i \int \mathcal{D}f_i \exp \left\{ -\frac{\mathcal{H}_{\text{tot}}[f_i, u]}{k_B T} \right. \\ &\quad \left. + i \int_{S_{i,\text{ref}}} d^2x \psi_i(\mathbf{x}) [u(\mathbf{x}) - f_{i,\text{ext}}(\mathbf{x})] \right\}. \end{aligned} \quad (28)$$

Similarly as with the evaluation of the fluctuation part (Sec. III), we introduce multipole moments Ψ_{im} of the auxiliary fields by inserting unity into \mathcal{Z} [Eq. (28)]:

$$\begin{aligned} 1 &= \int \prod_{i=1}^2 \prod_m d\Psi_{im}^c d\Psi_{im}^s \delta \\ &\quad \times \left(\Psi_{im}^c - \int_{S_{i,\text{ref}}} d^2x [\cosh(m\xi)/\cosh(m\xi_0)] \cos(m\eta) \psi_i(\mathbf{x}) \right) \\ &\quad \times \delta \left(\Psi_{im}^s - \int_{S_{i,\text{ref}}} d^2x [\sinh(m\xi)/\sinh(m\xi_0)] \sin(m\eta) \psi_i(\mathbf{x}) \right). \end{aligned} \quad (29)$$

In contrast to the evaluation of the fluctuation term in Sec. III, there will be constraints on the lowest multipoles which contribute to \mathcal{Z} . To see this we note that the Hamiltonian \mathcal{H}_{tot} does not depend on the boundary monopole moments P_{i0} and the dipole moments P_{i1} (through a cancellation between $\mathcal{H}_{i,\text{b}}$ and $\mathcal{H}_{i,\text{corr}}$), and the only dependence of \mathcal{Z} on these moments is through the constraint function $f_{i,\text{ext}}$. Recalling the definition of the integration measure $\mathcal{D}f_i$ for the two boundary conditions B and C and performing the integration over P_{i0} (B) and P_{i0} and P_{i1} (C), we immediately find

$$\mathcal{Z} \sim \begin{cases} \int \prod_{i=1}^2 \prod_m d\Psi_{im}^s d\Psi_{im}^c \cdots \delta(\Psi_{i0}^c) \cdots, & \text{case B} \\ \int \prod_{i=1}^2 \prod_m d\Psi_{im}^s d\Psi_{im}^c \cdots \delta(\Psi_{i0}^c) \delta(\Psi_{i1}^c) \delta(\Psi_{i1}^s) \cdots, & \text{case C.} \end{cases} \quad (30)$$

Having noticed these constraints on the auxiliary fields, we proceed by integrating over the field u in Eq. (28):

$$\begin{aligned} \mathcal{Z} = & \int \prod_{i=1}^2 \mathcal{D}\psi_i \int \mathcal{D}f_i \exp \left\{ -\frac{k_B T}{2\gamma} \sum_{i,j=1}^2 \int_{S_{i,\text{ref}}} d^2x_i \right. \\ & \times \int_{S_{j,\text{ref}}} d^2x_j \psi_i(\mathbf{x}_i) G(|\mathbf{x}_i - \mathbf{x}_j|) \psi_j(\mathbf{x}_j) - \frac{1}{k_B T} (\mathcal{H}_{i,b} + \mathcal{H}_{i,\text{corr}}) \\ & \left. - i \sum_{i=1}^2 \int_{S_{i,\text{ref}}} d^2x \psi_i(\mathbf{x}) f_{i,\text{ext}}(\mathbf{x}) \right\}, \quad (31) \end{aligned}$$

where—as in Eq. (10)— G is the Green's function of the capillary-wave Hamiltonian. A somewhat longer calculation shows that \mathcal{Z} can be split into an interaction part (coupling the auxiliary multipole moments $\Psi_{im}^{c[s]}$, P_{im} , and Q_{im} for different colloid labels i), a self-energy part (depending on $\Psi_{im}^{c[s]}$, P_{im} , and Q_{im} for each value of i separately), and a remainder (the sum of boundary and correction Hamiltonians):

$$\begin{aligned} \mathcal{Z} = & \int \prod_{i=1}^2 \prod_m d\Psi_{im}^c d\Psi_{im}^s \int \mathcal{D}f_i \exp \left\{ -\frac{k_B T}{2\gamma} (\mathcal{H}_{\text{int}}[\Psi_{1m}^{c[s]}, \Psi_{2m}^{c[s]}] \right. \\ & + \mathcal{H}_{i,\text{self}}[\Psi_{im}^{c[s]}]) \left. \right\} \exp \left(\frac{1}{k_B T} (\mathcal{H}_{i,b} + \mathcal{H}_{i,\text{corr}}) - i \sum_m (\Psi_{im}^c P_{im} \right. \\ & \left. + \Psi_{im}^s Q_{im}) \right). \quad (32) \end{aligned}$$

The interaction part

$$\mathcal{H}_{\text{int}} = 2 \int_{S_{1,\text{ref}}} d^2x_1 \int_{S_{2,\text{ref}}} d^2x_2 \psi_1(\mathbf{x}_1) G_{\text{int}}(|\mathbf{x}_1 - \mathbf{x}_2|) \psi_2(\mathbf{x}_2) \quad (33)$$

turns out to be a bilinear form in the auxiliary multipole moments. This is shown using the already used multipole expansion of the Green's function $G(|\mathbf{x}_1 - \mathbf{x}_2|) \approx -\ln(\gamma_e |\mathbf{x}_1 - \mathbf{x}_2| / 2\lambda_c)$ (valid for $d \gg a$), which is presented in Appendix C in more detail. This bilinear form reads

$$2\pi \mathcal{H}_{\text{int}} = \begin{pmatrix} \hat{\Psi}_1^c \\ \hat{\Psi}_1^s \end{pmatrix}^T \begin{pmatrix} \hat{\mathbf{G}}_{\text{int}}^{cc} & \hat{\mathbf{G}}_{\text{int}}^{sc} \\ \hat{\mathbf{G}}_{\text{int}}^{sc} & \hat{\mathbf{G}}_{\text{int}}^{ss} \end{pmatrix} \begin{pmatrix} \hat{\Psi}_2^c \\ \hat{\Psi}_2^s \end{pmatrix}, \quad (34)$$

where the submatrices $\hat{\mathbf{G}}_{\text{int}}^{cc}$, $\hat{\mathbf{G}}_{\text{int}}^{sc}$, and $\hat{\mathbf{G}}_{\text{int}}^{ss}$ have already been encountered in the calculation of the fluctuation part and are given by Eqs. (15)–(18). The self-energy part (different from the corresponding one in the calculation of the fluctuation

part) is evaluated in Appendix D, with the result

$$\begin{aligned} \mathcal{H}_{i,\text{self}} = & -\frac{\ln[\gamma_e(a+b)/8\lambda_c]}{2\pi} \Psi_{i0}^{c2} + \frac{1}{\pi} \sum_{m>0} \frac{1}{m} \left(\frac{\Psi_{im}^{c2}}{1 + \tanh(m\xi_0)} \right. \\ & \left. + \frac{\Psi_{im}^{s2}}{1 + \coth(m\xi_0)} \right). \quad (35) \end{aligned}$$

Combining Eqs. (32), (33), and (35), the partition function can be written as

$$\begin{aligned} \mathcal{Z} = & \int \prod_{i=1}^2 \prod_m \mathcal{D}\Psi_{im} \mathcal{D}f_i \exp \left\{ -\frac{k_B T}{2\gamma} \begin{pmatrix} \hat{\Psi}_1 \\ \hat{\Psi}_2 \end{pmatrix}^\dagger \begin{pmatrix} \hat{\mathbf{H}}_{\text{self}} & \hat{\mathbf{H}}_{\text{int}} \\ \hat{\mathbf{H}}_{\text{int}} & \hat{\mathbf{H}}_{\text{self}} \end{pmatrix} \right. \\ & \left. \times \begin{pmatrix} \hat{\Psi}_1 \\ \hat{\Psi}_2 \end{pmatrix} \right\}, \quad (36) \end{aligned}$$

where the vectors $\Psi_i = (\Psi_{i0}^c, P_{i0}, \Psi_{i1}^c, P_{i1}, \Psi_{i1}^s, Q_{i1}, \dots)$ —in contrast to $\hat{\Psi}_i$ in Sec. III—contain all involved auxiliary and boundary multipole moments. The elements of the matrix \mathbf{H} describe the coupling of these multipole moments, where the self-energy block couples multipoles defined on the same ellipses $S_{i,\text{ref}}$. Thus the diagonal part of the self-energy matrix $\hat{\mathbf{H}}_{\text{self}}$ can be read off Eqs. (26) and (35), while the off-diagonal part is determined by the term $-i \sum_m (\Psi_{im}^c P_{im} + \Psi_{im}^s Q_{im})$ in Eq. (32). The elements of the interaction matrix $\hat{\mathbf{H}}_{\text{int}}$ are determined by the interaction energy \mathcal{H}_{int} in Eqs. (33) and (34) and couple the auxiliary multipole moments of different colloids. All matrix elements representing couplings of other multipoles are zero. Similarly as in Eq. (12), the exponent in Eq. (36) is a bilinear form, but here combined for all types, boundary multipole moments P_{im} and Q_{im} and auxiliary multipoles Ψ_{im}^c and Ψ_{im}^s . The computation of the partition function amounts to the calculation of $\det \hat{\mathbf{H}}$. Again this is found as a series expansion in a/d . We may define a similar expansion for the free energy $\mathcal{F}_{\text{in+coll}} = -(k_B T) \ln \det \hat{\mathbf{H}}/2$ as before in Eq. (20):

$$\mathcal{F}_{\text{in+coll}}(d) = k_B T \sum_n f_{2n}^{\text{in+coll}} \left(\frac{1}{d} \right)^{2n}. \quad (37)$$

The leading coefficients in case B (inclusion of fluctuations in the ellipsoids' vertical positions) are given by

$$f_0^{\text{in+coll}} = f_2^{\text{in+coll}} = 0,$$

$$f_4^{\text{in+coll}} = -\frac{1}{2^8}[(a^2 - b^2)^2 \cos(2\theta_1 + 2\theta_2) + (a + b)^4]. \quad (38)$$

In case C (inclusion of fluctuations in the ellipsoids' vertical positions and tilt angles with respect to the interface) the leading coefficients are

$$f_{2n}^{\text{in+coll}} = 0, \quad n = 0, \dots, 3,$$

$$f_8^{\text{in+coll}} = -\frac{9}{2^{16}}[(a^2 - b^2)^4 \cos(4\theta_1 + 4\theta_2) + (a + b)^8]. \quad (39)$$

In contrast to the calculation before, the different leading power laws for the different cases B and C can be understood easily. We note that the interaction between the auxiliary multipoles $\Psi_{1m}^{(c,s)}$ and $\Psi_{2n}^{(c,s)}$ in \mathcal{H}_{int} [Eq. (33)] scales like $(a'/4d)^{m+n}$. After calculating the determinant, the leading order of the total fluctuation-induced force between the two colloids is determined by the first nonvanishing auxiliary multipole moment $\Psi_{im'}^{(c,s)}$ and (as follows from $\det \hat{\mathbf{H}}$) gives rise to a term in the free energy $\propto 1/d^{4m'}$ (for $m' > 0$) or $\propto \ln d$ (for $m' = 0$). As explained in the beginning of this subsection, the different boundary conditions lead to certain constraints on the auxiliary multipoles: according to Eq. (30), the leading term in $F(d)$ arises from a monopole-monopole interaction of the auxiliary field in case A, from a dipole-dipole interaction in case B, and from a quadrupole-quadrupole interaction in case C. The constraints of vanishing auxiliary monopole and dipole moments (as in C) result from the independence of \mathcal{H}_{tot} of the boundary monopole and dipole moments and this is only captured correctly by the inclusion of the correction Hamiltonian $\mathcal{H}_{\text{corr}}$. The Casimir attraction is maximal if the major axes of both ellipses are oriented parallel, regardless of the orientation of the distance vector joining their centers. This is a peculiarity in two dimensions, as can be seen also by the general multipole expansion of the interaction between two arbitrary charge distributions in two-dimensional electrostatics.

Limiting cases

In the limit $a=b$ (colloids with circular contact line such as disks and spheres), our results for cases A–C reduce to the results reported in Refs. [8,9]. In the limit $b \rightarrow 0$ (colloidal rods or needles with vanishing thickness), we can compare our result for case C (fluctuating colloid heights and tilts) to Ref. [7]. There it was found that the effective free energy asymptotically varies $\propto d^{-4}$ with a coefficient given by Eq. (38), i.e., by the result of case B (colloid height fluctuations only). The derivation in Ref. [7] suggests that the perturbative treatment employed in our approach should be amended by corrections in the integration measure over the tilts. In our cases, this measure is simply given by $dP_{i1}dQ_{i1}$, the product of the measures for the cosine and sine dipole moments of the contact line. In order to check the validity of this approximation for the measure, we recalculated the partition function of Ref. [7] by performing the integrations over the auxiliary dipole moments and their conjugate variables,

which results in a final integral over the tilts (with the general measure) weighted by an exponential function in the tilts. If $\gamma a^2/k_B T \gg 1$, the denominator of the measure in this integral can be expanded in terms of the tilt angles since the exponential function decays much faster than the measure and thus determines the convergence of the integral. In this way, one sees that the higher-order terms in the dipole tilt measure do not provide another leading behavior in $1/d$ in the partition function compared to the leading quadrupole-quadrupole interaction which arises in our perturbative picture. A breakdown of our perturbative treatment can be expected if the length of the rod a approaches the molecular length scale. This coincides with a simultaneous breakdown of the simple capillary-wave picture underlying our analysis.

V. SUMMARY

The restrictions that two colloids trapped at a fluid interface impose on the thermally excited interfacial fluctuations (capillary waves) by their sheer presence lead to a thermal Casimir interaction. We have obtained an explicit account of the effect of colloidal anisotropy on the form of the Casimir interaction by studying ellipsoidal (spheroidal) colloids with arbitrary aspect ratio. For the case of fixed colloids and fixed contact lines, the problem is equivalent to the standard Casimir problem for a scalar Gaussian field in two dimensions with Dirichlet boundary conditions on the colloid surface. In an expansion in $1/d$, the inverse center-to-center distance between the colloids, the leading term in the Casimir interaction energy is found to be attractive and isotropic in the interface plane and slowly varying as $\propto \ln d$ [see Eq. (21)]. Anisotropies appear in higher orders in $1/d$ and become important when the closest surface-to-surface distance between the colloids becomes small (see Fig. 3).

If fluctuations in the colloids' vertical position are permitted, the asymptotics of the Casimir interaction energy changes to a behavior $\propto d^{-4}$ [see Eq. (38)]. In this case, anisotropies are present in the leading term but the interaction remains attractive for all orientations. If furthermore fluctuations of the colloids' orientation with respect to the interface normal are allowed, the asymptotics changes to a behavior $\propto d^{-8}$ [see Eq. (39)]. Interestingly, this change in leading order in the asymptotics of the Casimir energy depending on the type of permitted colloid fluctuations holds for arbitrary aspect ratios. This leads to the speculation that this might be a general feature holding for arbitrary colloid shape.

In our approach, the Casimir interaction can be understood as the interaction between fluctuating multipole moments of an auxiliary charge-density-like field defined on the area enclosed by the contact lines. These fluctuations are coupled to fluctuations of multipole moments of the contact line position which are due to the possibly fluctuating colloid height and tilts. Therefore, the system can be viewed as an example of the Casimir effect with fluctuating boundary conditions. Such fluctuating boundary conditions appear to be difficult to be realizable in three-dimensional systems such as the standard system of charged metallic objects subjected to vacuum fluctuations of the electromagnetic field.

Experimentally, the detection of the Casimir interaction at a fluid interface appears to be possible if competing interactions, especially van der Waals and static capillary interactions, are sufficiently weakened. van der Waals interactions are also strongly attractive at small distances, but can be modified by an appropriate core-shell structure of the colloids or by using flat, disklike particles (we refer to a longer discussion of this issue in Ref. [8]). Capillary interactions are very strong for ellipsoidal colloids of micrometer size and with contact angle different from $\pi/2$ since the equilibrium contact line in this case is already undulated and gives rise to static deformations of the surrounding interface [21]. These capillary interactions can be minimized by either using truly nanoscopic ellipsoids or synthesizing Janus particles with a contact line which is flat on the nanometer level. Despite the great advances in particle synthesis over the last years, this appears to be still a big challenge.

ACKNOWLEDGMENT

The authors thank the German Science Foundation for financial support through the Collaborative Research Centre (SFB-TR6) ‘‘Colloids in External Fields,’’ Project No. N01.

APPENDIX A: CONFOCAL ELLIPTIC COORDINATE SYSTEM

Confocal elliptic coordinates (ξ, η) are planar orthogonal coordinates formed by confocal ellipses or hyperbolas. The foci are located on the x axis of the Cartesian coordinates, separated by a' . The relation to Cartesian coordinates is defined by

$$\begin{aligned} x &= \frac{a'}{2} \cosh(\xi) \cos(\eta), \\ y &= \frac{a'}{2} \sinh(\xi) \sin(\eta), \end{aligned} \quad (\text{A1})$$

and the scale factors are found as

$$h_\xi = h_\eta = \sqrt{\frac{a'^2}{2} [\cosh(2\xi) - \cos(2\eta)]}. \quad (\text{A2})$$

ξ and η are called elliptic radius and elliptic angle, respectively. In this coordinate system, $\xi = \xi_0$ represents the equation of an ellipse with axes a and b ($a > b$). The elliptic radius and the distance a' between the foci are given in terms of the ellipse principal axes by

$$\begin{aligned} \xi_0 &= \frac{1}{2} \ln \left(\frac{a+b}{a-b} \right), \\ a' &= (a^2 - b^2)^{1/2}. \end{aligned} \quad (\text{A3})$$

Therefore, for a circle we have $\xi_0 \rightarrow \infty$ and for a line, $\xi_0 \rightarrow 0$.

APPENDIX B: THE BOUNDARY AND CORRECTION HAMILTONIANS $\mathcal{H}_{i,b}$ AND $\mathcal{H}_{i,corr}$

(i) The boundary Hamiltonian for the case of a pinned contact line (Janus ellipsoids) is governed by the difference

in projected meniscus area, ΔA_{proj} [Eq. (2)]. If the ellipsoid is tilted in the xz plane by a small angle α_i , this area is given by

$$\Delta A_{\text{proj}}^{xz} \approx \frac{\pi}{16} \alpha_i^2 a'^2 \sinh(2\xi_0). \quad (\text{B1})$$

The contact line position $u|_{\partial S_{i,\text{ref}}}$ is easily determined by using a coordinate system rotation from the xz plane to the $x'z'$ plane, where the x' and the z' axes coincide with the major and minor axes of the tilted ellipsoid. The contact line is located at $z' = 0$ in the new coordinate system. Since $z' \approx z - \alpha_i x$, we find that $u|_{\partial S_{i,\text{ref}}} = z|_{z'=0} \approx \alpha_i x$ and therefore $u|_{\partial S_{i,\text{ref}}} \approx \alpha_i (a'/2) \cosh(\xi_0) \cos(\eta_i)$. Thus, in the multipole expansion of the tilted contact line [Eq. (3)], only a dipole term appears with the dipole moment given by

$$P_{i1} = \alpha_i \frac{a'}{2} \cosh(\xi_0). \quad (\text{B2})$$

Inserting Eq. (B2) into Eq. (B1) we obtain

$$\Delta A_{\text{proj}}^{xz} = \frac{\pi}{2} P_{i1}^2 \tanh(\xi_0). \quad (\text{B3})$$

Applying the same arguments for tilts in the yz plane, we can express the boundary Hamiltonian in the small-tilt approximation as

$$\mathcal{H}_{i,b} = \gamma \Delta A_{\text{proj}} = \frac{\gamma \pi}{2} [P_{i1}^2 \tanh(\xi_0) + Q_{i1}^2 \coth(\xi_0)]. \quad (\text{B4})$$

(ii) The correction Hamiltonian, which is introduced in Eq. (25), is determined by minus the surface energy of the meniscus piece $u|_{S_{i,\text{ref}}} \equiv f$ [Eq. (24)] extended into the ellipses enclosed by the reference contact lines:

$$-\mathcal{H}_{i,corr} = \frac{\gamma}{2} \int_{S_{i,\text{ref}}} d^2x \left[(\nabla u)^2 + \frac{u^2}{\lambda_c^2} \right]^{\lambda_c \rightarrow \infty} = \frac{\gamma}{2} \int d^2x (\nabla f)^2. \quad (\text{B5})$$

Thus,

$$\begin{aligned} -\mathcal{H}_{i,corr} &= \frac{\gamma}{2} \int_0^{\xi_0} \int_0^{2\pi} d\xi_i d\eta_i [(\partial_{\xi_i} f)^2 + (\partial_{\eta_i} f)^2] \\ &= \frac{\gamma \pi}{2} \sum_m m [P_{im}^2 \tanh(m\xi_0) + Q_{im}^2 \coth(m\xi_0)]. \end{aligned} \quad (\text{B6})$$

APPENDIX C: EXPANSION OF GREEN'S FUNCTION IN ELLIPTIC COORDINATES

In this appendix we derive the multipole expansion of the Green's function $G(|\mathbf{x}|) \approx -(1/2\pi) \ln(\gamma_c |\mathbf{x}| / 2\lambda_c)$ between two charged elliptic regions (charges are generated by auxiliary fields ψ_i). This Green's function gives the correlation between two points residing either on the same ellipse or different ellipses.

(1) In the case that \mathbf{x}_1 and \mathbf{x}_2 are located on the same ellipse, the Green's function expansion was given in Ref. [25]:

$$\begin{aligned}
2\pi G(|\mathbf{x}_1 - \mathbf{x}_2|) = & -\ln\left(\frac{\gamma_e a' e^{\xi_0}}{8\lambda_c}\right) \\
& + 2\sum_{n=1}^{\infty} \frac{e^{-n\xi_0}}{n} [\cosh(n\xi_0)\cos(n\eta_1)\cos(n\eta_2) \\
& + \sinh(n\xi_0)\sin(n\eta_1)\sin(n\eta_2)]. \quad (\text{C1})
\end{aligned}$$

(2) The case that the two points are located on different ellipses, i.e., $\mathbf{x}_1 = \mathbf{r}_1$ and $\mathbf{x}_2 = \mathbf{d} + \mathbf{r}_2$, which furthermore possess an arbitrary orientation in the plane (expressed by the angles θ_1 and θ_2 ; see Fig. 1) is more difficult. We start with a general Taylor expansion of the Green's function:

$$\begin{aligned}
& -\frac{1}{2\pi} \ln\left(\frac{\gamma_e |\mathbf{d} + \mathbf{r}_2 - \mathbf{r}_1|}{2\lambda_c}\right) \\
& = -\frac{1}{2\pi} \ln\left(\frac{\gamma_e d}{2\lambda_c}\right) \\
& \quad \times -\frac{1}{2\pi} \sum_{\substack{j_1, j_2=0 \\ j_1+j_2 \geq 1}} \frac{(-\mathbf{r}_1 \cdot \nabla)^{j_1} (\mathbf{r}_2 \cdot \nabla)^{j_2}}{j_1! j_2!} \ln r \Bigg|_{r=d}. \quad (\text{C2})
\end{aligned}$$

On the other hand, we can perform this expansion using complex variables $z = x + iy$. The expansion of the logarithm is given by

$$\ln(z - z') = \sum_{j=0}^{\infty} \frac{1}{j!} (-z' \partial_z)^j \ln z. \quad (\text{C3})$$

The real part of Eq. (C3) is the expansion of the real logarithm, of course:

$$\ln|\mathbf{r} - \mathbf{r}'| = \text{Re} \sum_{j=0}^{\infty} -\frac{1}{j} \frac{(z' z^*)^j}{|z|^{2j}}. \quad (\text{C4})$$

By comparing Eq. (C4) and the Taylor expansion of $\ln|\mathbf{r} - \mathbf{r}'|$ in real space as in Eq. (C2), we find

$$\frac{(-\mathbf{r}' \cdot \nabla)^j}{j!} \ln r = -\frac{1}{j} \text{Re} \frac{(z' z^*)^j}{|z|^{2j}}. \quad (\text{C5})$$

Introducing complex derivative operators $\zeta_- = \partial_z$ and $\zeta_+ = \partial_{z^*}$ and using $\zeta_+ \zeta_- \ln r = \zeta_- \zeta_+ \ln r = 0$, we have

$$\zeta_{\pm}^j \ln r = \zeta_{\pm}^j \ln|z| = \frac{1}{2} (-1)^{j-1} (j-1)! \begin{cases} z^j / |z|^{2j} \\ z^*{}^j / |z|^{2j} \end{cases}. \quad (\text{C6})$$

Identifying Eqs. (C5) and (C6) we obtain

$$\frac{(\mathbf{r}' \cdot \nabla)^j}{j!} \ln r = \frac{1}{j!} [(z^*{}^j \zeta_+^j + z'^j \zeta_-^j] \ln r. \quad (\text{C7})$$

By inserting Eq. (C7) into Eq. (C2), we find the Green's function expansion in terms of complex variables z_i ,

$$\begin{aligned}
G|\mathbf{x}_2 - \mathbf{x}_1| = & -\frac{1}{2\pi} \ln\left(\frac{\gamma_e d}{2\lambda_c}\right) \\
& + \frac{1}{2\pi} \sum_{\substack{j_1, j_2=0 \\ j_1+j_2 \geq 1}} \frac{(-1)^{j_2}}{j_1 + j_2} \binom{j_1 + j_2}{j_1} \frac{1}{d^{j_1+j_2}} \text{Re}[z_1^{j_1} z_2^{j_2}]. \quad (\text{C8})
\end{aligned}$$

This general expansion can be used in any coordinate system. In the special case of elliptic coordinates, $z = (a'/2)e^{-i\theta} \cosh(\xi + i\eta)$, where θ is the in-plane rotation angle of the ellipse's major axis with respect to a fixed x axis. (For the configuration of arbitrarily oriented ellipses, the x axis is given by the line joining their centers; see Fig. 1) In order to express Eq. (C8) in elliptic coordinates, one needs z^j which can be found by applying the binomial expansion:

$$z^j = \left(\frac{a' e^{-i\theta}}{4}\right)^j \sum_{k=0}^j \binom{j}{k} e^{(2k-j)(\xi+i\eta)}. \quad (\text{C9})$$

Using the above expansion, Eq. (C8) becomes

$$\begin{aligned}
G(|\mathbf{x}_1 - \mathbf{x}_2|) = & -\frac{1}{2\pi} \ln\left(\frac{\gamma_e d}{2\lambda_c}\right) \\
& + \frac{1}{2\pi} \sum_{\substack{j_1, j_2=0 \\ j_1+j_2 \geq 1}} \sum_{k_1=0}^{j_1} \sum_{k_2=0}^{j_2} \frac{(-1)^{j_2}}{j_1 + j_2} \binom{j_1 + j_2}{j_1} \binom{j_1}{k_1} \\
& \times \binom{j_2}{k_2} \left(\frac{a'}{4d}\right)^{j_1+j_2} \exp[\xi_1(2k_1 - j_1) \\
& + \xi_2(2k_2 - j_2)] \cos[j_1\theta_1 + j_2\theta_2 + \eta_1(j_1 - 2k_1) \\
& + \eta_2(j_2 - 2k_2)]. \quad (\text{C10})
\end{aligned}$$

The aim is to rewrite this fourfold sum over j_1, j_2, k_1, k_2 as an expansion into multipole coefficients $\cos(m\eta_1)\cos(n\eta_2)$ and $\sin(m\eta_1)\sin(n\eta_2)$, with $m, n \geq 0$. To that end, we define $m = |j_1 - 2k_1|$ and $n = |j_2 - 2k_2|$. The possibility that $j_i - 2k_i$ may be positive as well as negative makes it necessary to consider the following cases: (i) “ $m=0, n=0$,” (ii) “ $m=0, n \neq 0$ ” or “ $m \neq 0, n=0$,” and (iii) “ $m \neq 0, n \neq 0$.”

(i) $m=0, n=0$: Two auxiliary variables l_1, l_2 are introduced through $j_i = 2l_i$ and $k_i = l_i$ ($i=1, 2$). Such constrained sum in Eq. (C10) reduces to

$$\begin{aligned}
& \sum_{\substack{l_1, l_2=0 \\ l_1+l_2 \geq 0}} \frac{1}{2(l_1 + l_2)} \binom{2(l_1 + l_2)}{2l_1} \binom{2l_1}{l_1} \binom{2l_2}{l_2} \\
& \times \left(\frac{a'}{4d}\right)^{2(l_1+l_2)} \cos(2l_1\theta_1 + 2l_2\theta_2).
\end{aligned}$$

Relabeling $l = l_1 + l_2$ and $l' = l_1$, the above sum is rewritten as

$$\begin{aligned}
& \sum_{l=1}^l \sum_{l'=0}^l \frac{1}{2l} \binom{2l}{2l'} \binom{2l'}{l'} \binom{2(l-l')}{l-l'} \left(\frac{a'}{4d}\right)^{2l} \\
& \times \cos[2l'\theta_1 + 2(l-l')\theta_2]. \quad (\text{C11})
\end{aligned}$$

(ii) “ $m=0, n>0$.” Here, l_1 is introduced as above through $j_1=2l_1$ and $k_1=l_1$. We distinguish the two cases $j_2-2k_2>0$ and $j_2-2k_2<0$ via the choice of l_2 through $j_2=n+2l_2$ and $k_2=l_2$ vs $k_2=n+l_2$. Adding up these two cases in constrained sum (C10) and performing a relabeling analogous to the one leading to expression (C11) ($l=l_1+l_2, l'=l_1$), we obtain

$$\begin{aligned} & 2 \sum_{l=0}^l \sum_{l'=0}^l (-1)^n \frac{\Gamma(n+2l)}{l'^2(l-l')!(n+l-l')!} \left(\frac{a'}{4d}\right)^{n+2l} \\ & \times (\cos\{2l'\theta_1 + [n+2(l-l')]\theta_2\} \cosh(n\xi_2) \cos(n\eta_2) \\ & + \sin\{2l'\theta_1 + [n+2(l-l')]\theta_2\} \sinh(n\xi_2) \sin(n\eta_2)). \end{aligned} \quad (\text{C12})$$

Similarly we obtain for “ $m>0, n=0$ ”

$$\begin{aligned} & 2 \sum_{l=0}^l \sum_{l'=0}^l \frac{\Gamma(m+2l)}{l'!(l-l')!(m+l')!} \left(\frac{a'}{4d}\right)^{m+2l} \{ \cos[(m+2l')\theta_1 \\ & + 2(l-l')\theta_2] \cosh(m\xi_1) \cos(m\eta_1) \\ & + \sin[(m+2l')\theta_1 + 2(l-l')\theta_2] \sinh(m\xi_1) \sin(m\eta_1) \}. \end{aligned} \quad (\text{C13})$$

(iii) “ $m>0, n>0$.” Similarly as in the previous cases, j_1 and j_2 are introduced through $j_1=m+2l_1$ and $j_2=n+2l_2$. The four cases of possible sign combinations of j_i-2k_i ($i=1,2$) are taken into account by the relation sets “ $k_1=l_1, k_2=l_2$,” “ $k_1=l_1, k_2=n+l_2$,” “ $k_1=m+l_1, k_2=l_2$,” and “ $k_1=m+l_1, k_2=n+l_2$.” Adding up these four cases in constrained sum (C10) and taking advantage of the addition and subtraction relations between hyperbolic functions and then relabeling as before ($l=l_1+l_2, l'=l_1$), we find

$$\begin{aligned} & 4 \sum_{l=0}^l \sum_{l'=0}^l (-1)^n \frac{\Gamma(m+n+2l)}{(m+l')!l'!(n+l-l')!(l-l')!} \left(\frac{a'}{4d}\right)^{m+n+2l} \\ & \times [\cos(\Theta) \cosh(m\xi_1) \cos(m\eta_1) \cosh(n\xi_2) \cos(n\eta_2) \\ & + \sin(\Theta) \sinh(m\xi_1) \sin(m\eta_1) \sinh(n\xi_2) \sin(n\eta_2)], \end{aligned} \quad (\text{C14})$$

where $\Theta=(m+2l')\theta_1+[n+2(l-l')]\theta_2$.

The cases considered above may be combined into a single expression such that the 2D Green's function in elliptic coordinates reads

$$\begin{aligned} G(|\mathbf{x}_1 - \mathbf{x}_2|) = & -\frac{1}{2\pi} \ln\left(\frac{\gamma_e d}{2\lambda_c}\right) + \frac{1}{2\pi} \sum_{m,n,l=0}^{\infty} \left(\frac{a'}{4d}\right)^{m+n+2l} \\ & \times \{ A_{mnl}^c [\cos(m\eta_1) \cosh(m\xi_1) \cos(n\eta_2) \cosh(n\xi_2) \\ & - \sin(m\eta_1) \sinh(m\xi_1) \sin(n\eta_2) \sinh(n\xi_2)] \\ & + A_{mnl}^s [\sin(m\eta_1) \sinh(m\xi_1) \cos(n\eta_2) \cosh(n\xi_2) \\ & + \cos(m\eta_1) \cosh(m\xi_1) \sin(n\eta_2) \sinh(n\xi_2)] \}. \end{aligned} \quad (\text{C15})$$

In Eq. (C15), the coefficients $A_{mnl}^{(c)}$ are given by

$$A_{mnl}^{(c)} = A_{mnl}^{(s)}(\theta_1, \theta_2) = 2^{H_n+H_m} \sum_{l'=0}^l C_{ll'}^{mn} \begin{pmatrix} \cos(\Theta) \\ \sin(\Theta) \end{pmatrix}, \quad (\text{C16})$$

where H_j is the discrete step function $H_j=1-\delta_{j0}$, and

$$C_{ll'}^{mn} = (-1)^n \frac{\Gamma(m+n+2l)}{(m+l')!l'!(n+l-l')!(l-l')!}, \quad (\text{C17})$$

with $C_{00}^{00}=0$.

APPENDIX D: SELF-ENERGY IN THE CASE OF FLUCTUATING COLLOIDS

For fluctuating colloids, the self-energy part of the multipole-multipole interaction of the auxiliary fields Ψ_i was introduced in Eq. (32). Here we calculate it explicitly with a method similar to the one employed in Ref. [7]. As the starting point, we obtain from Eqs. (31) and (32) the following expression for $\mathcal{Z}_{i,\text{self}} = \exp(-\frac{k_B T}{2\gamma} \mathcal{H}_{i,\text{self}})$:

$$\begin{aligned} \mathcal{Z}_{i,\text{self}} = & \int \prod_{i=1}^2 \mathcal{D}\psi_i \delta\left(\Psi_{im}^c - \int_{S_i} d^2x [\cos(m\xi)/\cosh(m\xi_0)]\right. \\ & \times \cos(m\eta) \psi(\mathbf{x}) \left. \delta\left(\Psi_{im}^s - \int_{S_i} d^2x [\sinh(m\xi)/\right.\right. \\ & \times \sinh(m\xi_0)] \sin(m\eta) \psi(\mathbf{x}) \left. \right) \exp\left(i \sum_m (\Psi_{im}^c P_{im} \right. \\ & + \Psi_{im}^s Q_{im}) \exp\left(-\frac{k_B T}{2\gamma} \int_{S_i} d^2x \int_{S_i} d^2x' \psi_i(\mathbf{x}) \right. \\ & \times G(|\mathbf{x} - \mathbf{x}'|) \psi_i(\mathbf{x}) - i \int_{S_{i,\text{ref}}} d^2x \psi_i(\mathbf{x}) f_{i,\text{ext}}(\mathbf{x}) \left. \right). \end{aligned} \quad (\text{D1})$$

The δ functions in $\mathcal{Z}_{i,\text{self}}$ may be eliminated by introducing conjugate multipole moments $\tilde{\Psi}_{im}^c$ and $\tilde{\Psi}_{im}^s$ to the multipoles $\Psi_{im}^{(c)}$ of the auxiliary fields:

$$\begin{aligned} & \delta\left(\Psi_{im}^{(c)} - \int_{S_{i,\text{ref}}} d^2x \begin{pmatrix} \cosh(m\xi_i) \cos(m\eta_i) / \cosh(m\xi_0) \\ \sinh(m\xi_i) \sin(m\eta_i) / \sinh(m\xi_0) \end{pmatrix} \psi_i(\mathbf{x}_i)\right) \\ & = \int d\tilde{\Psi}_{im}^{(c)} \exp\left\{ i \tilde{\Psi}_{im}^{(c)} \left[\Psi_{im}^{(c)} \right. \right. \\ & \left. \left. - \int_{S_{i,\text{ref}}} d^2x \begin{pmatrix} \cosh(m\xi_i) \cos(m\eta_i) / \cosh(m\xi_0) \\ \sinh(m\xi_i) \sin(m\eta_i) / \sinh(m\xi_0) \end{pmatrix} \psi_i(\mathbf{x}_i) \right] \right\}. \end{aligned} \quad (\text{D2})$$

Inserting Eq. (D2) into $\mathcal{Z}_{i,\text{self}}$ we obtain

$$\begin{aligned}
\mathcal{Z}_{i,\text{self}} = & \int \prod_m d\tilde{\Psi}_{im} \int \mathcal{D}\psi_i \exp\left(-\frac{k_B T}{2\gamma} \int_{S_{i,\text{ref}}} d^2x \right. \\
& \times \int_{S_{i,\text{ref}}} d^2x' \psi_i(\mathbf{x}_i) G(|\mathbf{x} - \mathbf{x}'|) \psi_i(\mathbf{x}_i) - i \int_{S_{i,\text{ref}}} d^2x \psi_i(\mathbf{x}_i) \\
& \times \left[\sum_m \frac{\cosh(m\xi_i)}{\cosh(m\xi_0)} (P_{im} + \tilde{\Psi}_{im}^c) \cos(m\eta_i) \right. \\
& \left. \left. + \frac{\sinh(m\xi_i)}{\sinh(m\xi_0)} (Q_{im} + \tilde{\Psi}_{im}^s) \sin(m\eta_i) \right] + i \sum_{m=0} [(P_{im} \right. \\
& \left. + \tilde{\Psi}_{im}^c) \Psi_{im}^c + (Q_{im} + \tilde{\Psi}_{im}^s) \Psi_{im}^s] \right), \quad (\text{D3})
\end{aligned}$$

where $d\tilde{\Psi}_{im} = d\tilde{\Psi}_{im}^s d\tilde{\Psi}_{im}^c$. The functional integral $\int \mathcal{D}\psi_i$ in Eq. (D3) can be replaced by a functional integral over a constrained height field $h(\mathbf{x})$:

$$\begin{aligned}
\mathcal{Z}_{i,\text{self}} = & \int \prod_m d\tilde{\Psi}_{im} \exp\left(i \sum_{m=0} [(P_{im} + \tilde{\Psi}_{im}^c) \Psi_{im}^c \right. \\
& \left. \times + (Q_{im} + \tilde{\Psi}_{im}^s) \Psi_{im}^s] \right) \int \mathcal{D}h \prod_{\mathbf{x}_i \in S_{i,\text{ref}}} \delta(h(\mathbf{x}_i) - \tilde{f}_i) \\
& \times \exp\left(-\frac{\gamma}{2k_B T} \int d^2x \left[(\nabla h)^2 + \frac{h^2}{\lambda_c^2} \right] \right), \quad (\text{D4})
\end{aligned}$$

where $\tilde{f}_i = \sum_m \{ [\cosh(m\xi_i)/\cosh(m\xi_0)] (P_{im} + \tilde{\Psi}_{im}^c) \cos(m\eta_i) + [\sinh(m\xi_i)/\sinh(m\xi_0)] (Q_{im} + \tilde{\Psi}_{im}^s) \sin(m\eta_i) \}$.

In the region $S_{i,\text{ref}}$, i.e., the ellipse enclosed by the reference contact line, the height field h is pinned to \tilde{f}_i . Therefore the contribution of the functional integral $\int \mathcal{D}h$ in this region is simply given by the surface energy of \tilde{f}_i which was determined in Eq. (B6) and $\mathcal{Z}_{i,\text{self}}$ becomes

$$\begin{aligned}
\mathcal{Z}_{i,\text{self}} \stackrel{\lambda_c \rightarrow \infty}{\approx} & \int \prod_m d\tilde{\Psi}_{im} \exp\left(-\frac{\gamma\pi}{2k_B T} \sum_m m [(P_{im} \right. \\
& \left. + \tilde{\Psi}_{im}^c)^2 \tanh(m\xi_0) + (Q_{im} + \tilde{\Psi}_{im}^s)^2 \coth(m\xi_0)] \right. \\
& \left. + i \sum_m [(P_{im} + \tilde{\Psi}_{im}^c) \Psi_{im}^c + (Q_{im} + \tilde{\Psi}_{im}^s) \Psi_{im}^s] \right) \\
& \times \int \mathcal{D}h \prod_{\mathbf{x}_i \in \partial S_{i,\text{ref}}} \delta(h(\mathbf{x}_i) - \tilde{f}_i) \\
& \times \exp\left(-\frac{\gamma}{2k_B T} \int_{\mathbb{R}^2 \setminus S_{i,\text{ref}}} d^2x \left[(\nabla h)^2 + \frac{h^2}{\lambda_c^2} \right] \right), \quad (\text{D5})
\end{aligned}$$

where the remaining δ functions describe the pinning of $h(\mathbf{x})$ to the boundaries $\partial S_{i,\text{ref}}$ of the integration domain. The auxiliary field can be separated into two parts, $h = h_0 + h_1$, where

$(-\nabla + \lambda_c^{-2})h_0 = 0$ with the boundary conditions $h_0(\mathbf{x}_i)|_{\partial S_{i,\text{ref}}} \equiv \tilde{f}_i$ and $h_1(\mathbf{x}_i)|_{\partial S_{i,\text{ref}}} = 0$. Applying Gauss's theorem to the integral in the exponent of Eq. (D5) leads to

$$\begin{aligned}
\mathcal{Z}_{i,\text{self}} = & \int \prod_m d\tilde{\Psi}_{im} \exp\left(-\frac{\gamma\pi}{2k_B T} \sum_m m [(P_{im} + \tilde{\Psi}_{im}^c)^2 \tanh(m\xi_0) \right. \\
& \left. + (Q_{im} + \tilde{\Psi}_{im}^s)^2 \coth(m\xi_0)] + i \sum_m [(P_{im} + \tilde{\Psi}_{im}^c) \Psi_{im}^c \right. \\
& \left. + (Q_{im} + \tilde{\Psi}_{im}^s) \Psi_{im}^s] \right) \exp\left(-\frac{\gamma}{2k_B T} \oint d\mathbf{x} h_0(\mathbf{x}) \nabla h_0(\mathbf{x}) \right) \\
& \times \int \mathcal{D}h_1 \prod_{\mathbf{x}_i \in S_{i,\text{ref}}} \delta(h_1(\mathbf{x}_i)) \\
& \times \exp\left(-\frac{\gamma}{2k_B T} \int_{\mathbb{R}^2 \setminus S_{i,\text{ref}}} d^2x \left[(\nabla h_1)^2 + \frac{h_1^2}{\lambda_c^2} \right] \right). \quad (\text{D6})
\end{aligned}$$

The functional integral over h_1 yields a constant value independent of any multipole moment, which can be neglected.

The general solution to the Helmholtz differential equation for h_0 in $\mathbb{R}^2 \setminus S_{i,\text{ref}}$ is needed for computing the line integral in Eq. (D6). Separation of variables in the Helmholtz equation in elliptic coordinates would lead to the Mathieu (angular part) and modified Mathieu (radial part) differential equations. The solution to these equations in the asymptotic case $\lambda_c \rightarrow \infty$ become standard trigonometric functions (angular part) and modified Bessel functions of the second kind (radial part), respectively. Therefore, the solution is given by

$$h_0(\mathbf{x}_i) = \sum_m \frac{K_m(a' e^{\xi_i/2\lambda_c})}{K_m(a' e^{\xi_0/2\lambda_c})} [A_m \cos(m\eta_i) + B_m \sin(m\eta_i)]. \quad (\text{D7})$$

The coefficients in Eq. (D7) are readily determined by comparing to the boundary conditions: $A_m = P_{im} + \tilde{\Psi}_{im}^c$, $B_m = Q_{im} + \tilde{\Psi}_{im}^s$, and $B_0 = 0$. Then the line integral evaluates to $2\pi g(m)(A_m^2 + B_m^2)$, with $g(m) = m/2$ ($m > 0$) and $g(0) = -1/\ln(\gamma_e a' e^{\xi_0/8\lambda_c})$. Using this, $\mathcal{Z}_{i,\text{self}}$ reads

$$\begin{aligned}
\mathcal{Z}_{i,\text{self}} = & \int \prod_m d\tilde{\Psi}_{im} \exp\left(-\frac{\gamma\pi}{2k_B T} \sum_m m [(P_{im} + \tilde{\Psi}_{im}^c)^2 \tanh(m\xi_0) \right. \\
& \left. + (Q_{im} + \tilde{\Psi}_{im}^s)^2 \coth(m\xi_0)] \right. \\
& \left. + i \sum_m [(P_{im} + \tilde{\Psi}_{im}^c) \Psi_{im}^c + (Q_{im} + \tilde{\Psi}_{im}^s) \Psi_{im}^s] \right) \\
& \times \exp\left(-\frac{\gamma\pi}{k_B T} \sum_{m=0} g(m) [(P_{im} + \tilde{\Psi}_{im}^c)^2 \right. \\
& \left. + (Q_{im} + \tilde{\Psi}_{im}^s)^2] \right). \quad (\text{D8})
\end{aligned}$$

The last integration over the conjugate multipole moments can be performed after shifting variables, $\tilde{\Psi}_{im}^c \rightarrow P_{im} + \tilde{\Psi}_{im}^c$ and $\tilde{\Psi}_{im}^s \rightarrow Q_{im} + \tilde{\Psi}_{im}^s$. After this integration, the final result for $\mathcal{H}_{i,\text{self}} = (-2\gamma)/(k_B T) \ln \mathcal{Z}_{i,\text{self}}$ is given by

$$\mathcal{H}_{i,\text{self}} = -\frac{\ln(\gamma_e a' e^{\xi_0/8\lambda_c})}{2\pi} \Psi_{i0}^{c2} + \frac{1}{\pi} \sum_{m>0} \frac{1}{m} \left(\frac{\Psi_{im}^{c2}}{1 + \tanh(m\xi_0)} + \frac{\Psi_{im}^{s2}}{1 + \coth(m\xi_0)} \right). \quad (\text{D9})$$

-
- [1] M. Kardar and R. Golestanian, *Rev. Mod. Phys.* **71**, 1233 (1999).
- [2] H. B. G. Casimir, *Proc. K. Ned. Akad. Wet.* **51**, 793 (1948).
- [3] K. A. Milton, *J. Phys. A* **37**, R209 (2004).
- [4] M. E. Fisher and P. G. de Gennes, *C. R. Seances Acad. Sci., Ser. B* **287**, 207 (1978).
- [5] C. Hertlein, L. Helden, A. Gambassi, S. Dietrich, and C. Bechinger, *Nature (London)* **451**, 172 (2008).
- [6] M. Goulian, R. Bruinsma, and P. Pincus, *Europhys. Lett.* **22**, 145 (1993); **23**, 155(E) (1993).
- [7] R. Golestanian, M. Goulian, and M. Kardar, *Phys. Rev. E* **54**, 6725 (1996).
- [8] H. Lehle, M. Oettel, and S. Dietrich, *Europhys. Lett.* **75**, 174 (2006).
- [9] H. Lehle and M. Oettel, *Phys. Rev. E* **75**, 011602 (2007).
- [10] H. Lehle and M. Oettel, *J. Phys.: Condens. Matter* **20**, 404224 (2008).
- [11] T. Emig, N. Graham, R. L. Jaffe, and M. Kardar, *Phys. Rev. D* **77**, 025005 (2008).
- [12] T. Emig, N. Graham, R. L. Jaffe, and M. Kardar, *Phys. Rev. Lett.* **99**, 170403 (2007).
- [13] R. Büscher and T. Emig, *Phys. Rev. A* **69**, 062101 (2004).
- [14] B. Döbrich, M. DeKieviet, and H. Gies, *Phys. Rev. D* **78**, 125022 (2008).
- [15] H. Gies and K. Klingmüller, *Phys. Rev. Lett.* **97**, 220405 (2006).
- [16] K. A. Milton, P. Parashar, and J. Wagner, *Phys. Rev. Lett.* **101**, 160402 (2008).
- [17] T. Emig, N. Graham, R. L. Jaffe, and M. Kardar, arXiv:0811.1597.
- [18] D. Jasnow, in *Phase Transitions and Critical Phenomena*, edited by C. Domb and J. L. Lebowitz (Academic, London, 1986), Vol. 10.
- [19] M. Oettel, A. Dominguez, and S. Dietrich, *Phys. Rev. E* **71**, 051401 (2005).
- [20] S. Safran, *Statistical Thermodynamics of Surfaces, Interfaces, and Membranes* (Westview, Boulder, 1994).
- [21] H. Lehle, E. Noruzifar, and M. Oettel, *Eur. Phys. J. E* **26**, 151 (2008).
- [22] B. Derjaguin, *Kolloid-Z.* **69**, 155 (1934).
- [23] H. Li and M. Kardar, *Phys. Rev. Lett.* **67**, 3275 (1991).
- [24] W. H. Press, S. A. Teukolsky, W. T. Vetterling, and B. P. Flannery, *Numerical Recipes in C++*, 2nd ed. (Cambridge University Press, Cambridge, England, 2002).
- [25] P. M. Morse and H. Feshbach, *Methods of Theoretical Physics* (McGraw-Hill, New York, 1953), p. 1202.